J Nanostruct 15(3): 1380-1393, Summer 2025

RESEARCH PAPER

Fe_3O_4-ZnO Incorporated in Chitosan-Carbon Nanotubes (Fe_3O_4-ZnO-CHIT-CNT) as a Hybrid Organic Inorganic Biodegradable Nano-composites for Application in Bone Tissue Engineering

Vays Juraev [1], Kamol Xakimov [2], Dilafruz Khakimova [3], Ibrokhimjon N. Abdullayev [4,1], Ikrom Nasimov [5], Nargiza Muminova [6], Uktam Fozilov [7], Jonibek Durdiev [7], Azamat Niyazmetov [8], Dildora Israilova [9], Soxiba Narkulova [10], Sojida Raupova [11], Ogiloy Bozorova [12]

[1] *Tashkent State Technical University named after Islam Karimov, Tashkent, Uzbekistan*

[2] *Termez State University of Engineering and Agrotechnology, Termez, Uzbekistan*

[3] *Almalyk branch of Tashkent State Technical University, Uzbekistan*

[4] *Professional Development Center for Medical Workers, Tashkent, Uzbekistan*

[5] *Samarkand State University named after Sharof Rashidov, Samarkand, Uzbekistan*

[6] *Jizzakh State Pedagogical university, Uzbekistan*

[7] *Bukhara State Medical Institute, 23, Gijduvanskaya str, Bukhara city, 200118, Uzbekistan*

[8] *Urgench State University, Uzbekistan*

[9] *Tashkent Institute of Irrigation and Agricultural Mechanization Engineers National Research University, Tashkent, Uzbekistan*

[10] *Samarkand State Medical University, Samarkand, Uzbekistan*

[11] *Termez State Pedagogical Institute, Termez, Uzbekistan*

[12] *Chirchik State Pedagogical University, Tashkent Region, Chirchik city, Uzbekistan*

ARTICLE INFO

Article History:
Received 06 April 2025
Accepted 28 June 2025
Published 01 July 2025

Keywords:
Bone tissue engineering
Carbon nanotube
Chitosan
Inorganic-organic
Nanocomposites

ABSTRACT

Bone tissue engineering seeks innovative solutions to address critical-sized bone defects that surpass the body's natural regenerative capacity. In this study, we developed a novel hybrid nanocomposite integrating Fe_3O_4 and ZnO nanoparticles within a chitosan-carbon nanotube (CNT) matrix to serve as an effective scaffold for bone regeneration. The synthesis involved functionalization of CNTs, formation of inorganic nanostructures, and their precise incorporation into a biodegradable chitosan matrix, resulting in a hierarchically structured, biocompatible material. Extensive characterization confirmed the successful embedding of inorganic phases and the preservation of crystalline integrity, with FE-SEM revealing uniform nanostructure distribution, FT-IR identifying chemical interactions, and XRD confirming phase purity. Biological assessments demonstrated high cytocompatibility and enhanced osteogenic activity, supported by cell viability, proliferation, ALP activity, and mineralization results. Mechanical testing indicated excellent load-bearing properties, while in vitro bioactivity assays showed significant apatite formation. The scaffold exhibited sustained biodegradability and maintained a physiological pH during degradation. These findings suggest that Fe_3O_4-ZnO-CHIT-CNT nanocomposites possess promising potential as multifunctional, biodegradable scaffolds for effective bone tissue regeneration, paving the way for future clinical applications in regenerative medicine.

How to cite this article
Juraev V., Xakimov K., Khakimova D et al. Fe_3O_4-ZnO Incorporated in Chitosan-Carbon Nanotubes (Fe_3O_4-ZnO-CHIT-CNT) as a Hybrid Organic Inorganic Biodegradable Nano-composites for Application in Bone Tissue Engineering. J Nanostruct, 2025; 15(3):1380-1393. DOI: 10.22052/JNS.2025.03.053

* *Corresponding Author Email: ways-j1978@mail.ru*

INTRODUCTION

Bone tissue engineering has emerged as a revolutionary approach within regenerative medicine, aiming to address critical-sized bone defects that surpass the natural regenerative capacity of the body [1-3]. Historically, efforts in this field date back to the late 20th century, driven by the increasing demand for effective treatments for bone loss resulting from trauma, degenerative diseases, and congenital anomalies [4-6]. The foundational concept involves the integration of scaffold materials [7], cellular components [8, 9], and bioactive molecules [10, 11] to mimic the native bone extracellular matrix and facilitate osteogenesis. Over the years, the field has expanded to encompass diverse strategies such as scaffold design optimization, stem cell therapy, and the incorporation of nanomaterials to enhance structural and biological functionalities (Fig. 1). These advancements have significantly improved the prospects for functional bone regeneration, with particular attention given to achieving biomimicry at the nanoscale, promoting cellular adhesion, proliferation, and differentiation [12-16]. The multidisciplinary nature of bone tissue engineering continues to evolve, combining principles from materials science [17, 18], biology [19], and chemistry [20] to develop innovative solutions for clinical challenges in skeletal reconstruction.

The integration of nanomaterials into bone tissue engineering represents a transformative advancement, leveraging the unique physicochemical properties at the nanoscale to emulate the hierarchical architecture of native bone tissue [21, 22]. Nanomaterials such as metal oxides [23], carbon nanotubes [24], and biocompatible polymers [25, 26] offer significant benefits, including enhanced surface area, improved mechanical strength, and tunable bioactivity, which facilitate cellular adhesion, proliferation, and differentiation. The development of nanocomposites hybrid materials composed of organic matrices reinforced with inorganic nanoparticles has emerged as a promising strategy to address the complex demands of bone regeneration [27-29]. These nanocomposites harness the synergistic effects of their constituents, combining the biocompatibility and biodegradability of organic

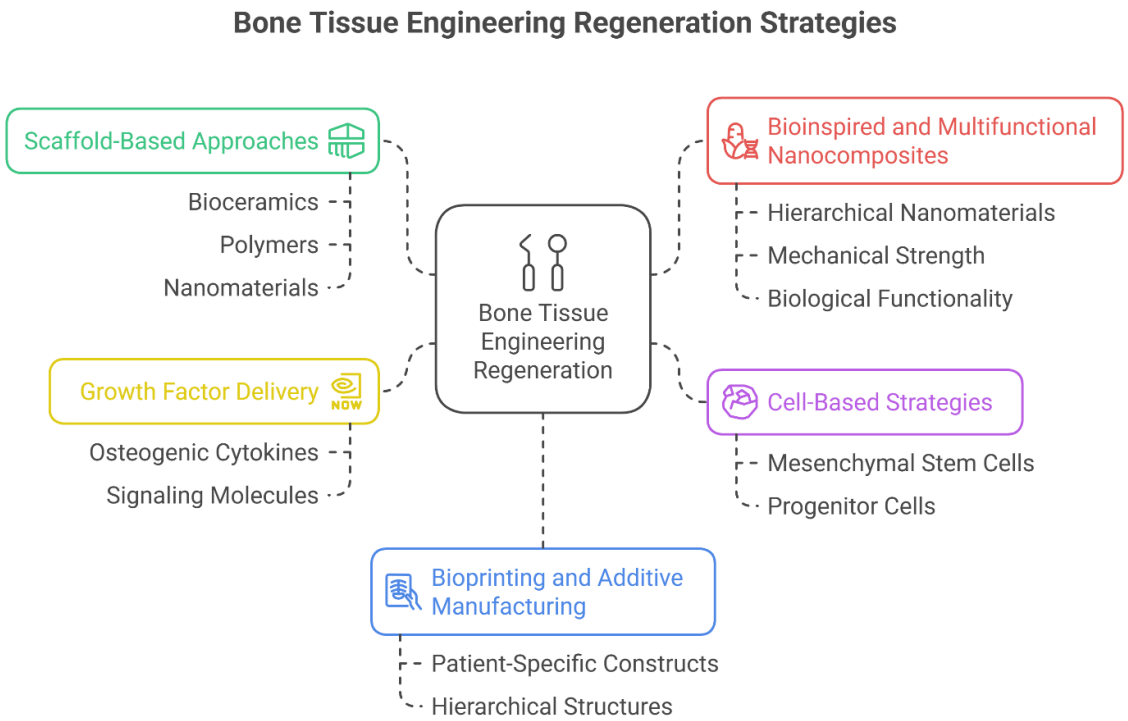

Fig. 1. Different types of bone tissue engineering regeneration methods.

polymers like chitosan with the osteoconductive and antimicrobial properties of inorganic nanomaterials such as Fe_3O_4 and ZnO. Such multifunctional nanostructured systems not only mimic the natural extracellular matrix at the nanoscale but also provide enhanced mechanical robustness and biological functionality, thereby paving the way for more effective and sustainable solutions in bone tissue repair and regeneration.

Recent advances in bone tissue engineering have prominently featured the incorporation of nanomaterials and nanocomposite systems designed to replicate the complex hierarchical structure of native bone and enhance regenerative outcomes. Notable systems include hydroxyapatite (HA) nanocrystals [30, 31], bioactive glass nanoparticles [32], carbon nanotubes (CNTs) [33], and metal oxide-based nanostructures such as Fe_3O_4 [34] and ZnO [35], which have shown promise due to their high surface area, osteoconductivity, and antimicrobial properties. For instance, hydroxyapatite/polymer nanocomposites [36, 37] have proven effective in promoting mineralization and cellular adhesion, while CNT-reinforced biodegradable matrices offer superior mechanical strength essential for load-bearing applications [38-40]. Recent developments have also introduced magneto-responsive nanocomposites, such as Fe_3O_4-ZnO embedded in chitosan matrices, enabling targeted delivery and stimulation. These systems afford substantial benefits, including improved bioactivity, enhanced mechanical properties, and multifunctionality; however, challenges such as potential cytotoxicity, immune responses, and difficulties in achieving uniform dispersion of nanomaterials persist. The trade-offs between biocompatibility and mechanical or functional enhancements remain a key area of ongoing research, underscoring the importance of optimizing nanomaterial surface modifications and composite fabrication techniques to balance efficacy and safety in clinical applications. Fig. 2 shows nanomaterials used in bone tissue engineering regeneration.

The primary aim of this study is to develop and characterize a novel hybrid organic-inorganic nanocomposite comprising Fe_3O_4 and ZnO nanoparticles embedded within a chitosan-carbon nanotube (CNT) matrix, tailored for bone tissue engineering applications. The research will focus on synthesizing these nanocomposites, evaluating their physicochemical properties, biocompatibility, and biodegradability. Furthermore, comprehensive analyses will be conducted to assess their structural, mechanical, and bioactive features, alongside in vitro evaluations of cellular responses. This work aspires to demonstrate the potential of these multifunctional nanocomposites as promising scaffolds for enhancing bone regeneration, leveraging the synergistic effects of magnetic, antimicrobial, and osteoconductive properties inherent to the constituent nanomaterials.

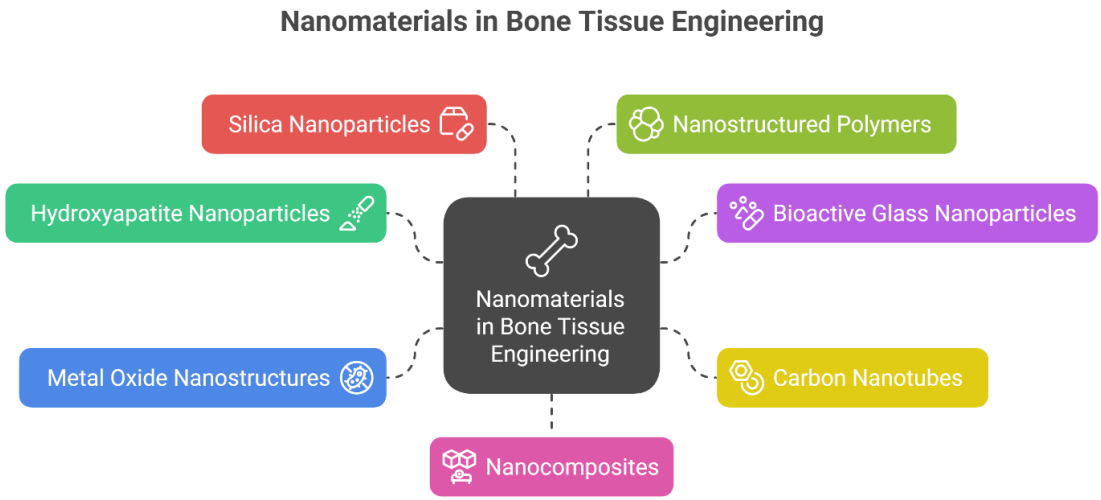

Fig. 2. Different types of nanomaterials in bone tissue engineering regeneration.

MATERIALS AND METHODS

The chemicals and apparatus

All chemicals and reagents utilized in this study were of analytical grade and procured from reputable suppliers. Chitosan (medium molecular weight, 75-85% deacetylated) was obtained from Sigma-Aldrich (CAS: 9012-76-4). Zinc acetate dihydrate (CAS: 27799-03-3), ferrous sulfate heptahydrate (CAS: 7782-63-0), zinc nitrate hexahydrate (CAS: 55566-31-1), and other inorganic precursors were purchased from Merck (Darmstadt, Germany). Multi-walled carbon nanotubes (MWCNTs, purity >95%, diameter 10-20 nm, length 10-30 µm) were supplied by Nanostructured and Amorphous Materials Inc.

The primary characterization tools employed included a Field Emission Scanning Electron Microscope (FE-SEM, Model: JEOL JSM-7900F, JEOL Ltd., Tokyo, Japan) for morphological analysis and surface topography. Fourier Transform Infrared Spectroscopy (FT-IR) was conducted using a Bruker Tensor II spectrometer (Bruker Corporation, Billerica, MA, USA) equipped with an attenuated total reflectance (ATR) accessory, operating within a spectral range of 4000–400 cm^{-1} to identify characteristic functional groups and confirm composite formation. All measurements were performed under standard conditions unless otherwise specified, with spectral data processed using OPUS software (Bruker). The FE-SEM imaging was performed at an accelerating voltage of 15 kV, while FT-IR spectra were acquired with a resolution of 4 cm^{-1}, averaging 32 scans per sample for optimal data quality. Furthermore, X-ray diffraction (XRD) analysis was carried out using a Bruker D8 Advance diffractometer (Bruker Corporation, Billerica, MA, USA) with Cu Kα radiation (λ = 1.5406 Å). The diffraction patterns were recorded over a 2θ range of 10°–80° at a scanning rate of 0.02° per second to evaluate the crystalline phases and structural properties of the synthesized nanocomposites.

Preparation of Fe_3O_4-ZnO Incorporated in Chitosan-Carbon Nanotubes (Fe_3O_4-ZnO-CHIT-CNT) Nanocomposites

The synthesis began with the dispersion of multi-walled carbon nanotubes (MWCNTs) in an aqueous solution. Precisely, 0.5 g of MWCNTs was ultrasonicated in 100 mL of distilled water containing 0.1 M of nitric acid for 2 hours to introduce functional groups and improve dispersibility. The acid-treated CNTs were then washed thoroughly with deionized water until neutral pH was achieved and subsequently dried at 60 °C [41, 42].

Concurrently, chitosan (0.5 g) was dissolved in 100 mL of 1% (v/v) acetic acid solution under magnetic stirring at room temperature until a clear, viscous solution was obtained. In another beaker, a mixture of Fe_3O_4 and ZnO nanoparticles prepared via co-precipitation and sol-gel methods respectively was dispersed in 50 mL of deionized water. To synthesize Fe_3O_4 nanoparticles, ferric chloride ($FeCl_3 \cdot 6H_2O$) and ferrous sulfate ($FeSO_4 \cdot 7H_2O$) were mixed in a molar ratio of 2:1, and the solution was heated to 70°C with stirring. Aqueous ammonia was then added dropwise until pH reached approximately 10, precipitating Fe_3O_4. After centrifugation, the Fe_3O_4 nanoparticles were washed with deionized water and dried at 60 °C. For ZnO, zinc acetate dihydrate was dissolved in ethanol and hydrolyzed by adding sodium hydroxide solution under stirring, followed by stirring at room temperature for 4 hours to obtain ZnO nanoparticles [43, 44].

Next, the Fe_3O_4 and ZnO nanoparticles were combined in a 1:1 molar ratio and dispersed in 50 mL of deionized water, facilitating the formation of the hybrid inorganic phase. This mixture was sonicated for 30 minutes to ensure uniformity.

The functionalized CNTs were then gradually added to the chitosan solution under vigorous magnetic stirring, maintaining gentle heating at 40 °C for 2 hours to ensure homogeneous dispersion and interaction. Subsequently, the Fe_3O_4-ZnO hybrid nanostructures were slowly introduced to the chitosan-CNT suspension, and the entire mixture was stirred continuously at 40 °C for an additional 4 hours to promote robust interaction and composite formation.

Finally, the resulting mixture was cast into petri dishes and dried at ambient temperature for 24 hours, followed by vacuum drying at 50 °C for 12 hours to remove residual solvents. The dried films were then ground into fine powders, which were stored in desiccators for further characterization and application testing.

Evaluation of Physicochemical Properties, Biocompatibility, and Biodegradability of Fe_3O_4-ZnO-CHIT-CNT Nanocomposites

The physicochemical characterization of the synthesized Fe_3O_4-ZnO-CHIT-CNT nanocomposites

was conducted to determine their structural, morphological, and compositional attributes. X-ray diffraction (XRD) analysis was performed using a Bruker D8 Advance diffractometer (Cu Kα radiation, λ = 1.5406 Å) over a 2θ range of 10° to 80°, with a scanning rate of 0.02°/s to evaluate the crystalline phases and estimate particle sizes via the Scherrer equation. Surface morphology was examined through field emission scanning electron microscopy (FE-SEM, Model: JEOL JSM-7900F, accelerating voltage 15 kV), providing insights into the nanostructure and dispersion qualities of inorganic components within the organic matrix. Surface functional groups and chemical interactions were analyzed through Fourier Transform Infrared Spectroscopy (FT-IR) using a Bruker Tensor II spectrometer (spectral range: 4000–400 cm^{-1}, resolution: 4 cm^{-1}, 32 scans per sample).

Biocompatibility was assessed via in vitro cytotoxicity tests following ISO 10993 standards. Human osteoblast-like cells (MG-63) were cultured in Dulbecco's Modified Eagle Medium (DMEM) supplemented with 10% fetal bovine serum at 37°C under 5% CO_2. Cell viability after 24, 48, and 72 hours of exposure to the nanocomposite extracts was determined using the MTT assay, with absorbance measured at 570 nm using a Thermo Scientific Multiskan FC microplate reader.

For biodegradability analysis, weight loss measurements were performed under simulated physiological conditions. Dried nanocomposite samples (about 50 mg) were immersed separately in phosphate-buffered saline (PBS, pH 7.4) at 37°C. At pre-determined intervals (1, 7, 14, 21, and 28 days), samples were removed, washed with distilled water, dried at 50°C until constant weight, and weighed. The percentage of weight loss was calculated to determine degradation rates. Additionally, pH variations of the PBS solution during degradation were monitored using a calibrated pH meter (Mettler Toledo SevenMulti), to evaluate the material's effect on surrounding biological fluids.

Assessment of Mechanical, Bioactive, and Cellular Response Properties of Fe_3O_4-ZnO-CHIT-CNT Nanocomposites

The mechanical properties of the fabricated Fe_3O_4-ZnO-CHIT-CNT nanocomposites were analyzed through a universal testing machine (UTM, Instron 3345, Norwood, MA, USA) under compression mode, with a crosshead speed of 1 mm/min. Samples were molded into standardized cylindrical shapes (diameter: 6 mm; height: 12 mm), and the compressive strength and Young's modulus were calculated from the stress-strain curves. For bioactivity assessment, the nanocomposites were immersed in simulated body fluid (SBF) prepared according to Kokubo's protocol at 37°C for periods of 7, 14, and 28 days. Post-immersion, the samples were gently rinsed, dried, and examined using FE-SEM to evaluate apatite formation on their surfaces, and the calcium and phosphate contents were quantified using energy-dispersive X-ray spectroscopy (EDS) coupled with SEM.

In vitro cellular responses were evaluated using human osteoblast-like MG-63 cells. Cells were seeded onto the nanocomposite samples at a density of 1×10^4 cells per well in 24-well plates and cultured in DMEM supplemented with 10% FBS at 37°C in a humidified incubator with 5% CO_2. Cell viability and proliferation were assessed after 1, 3, and 7 days via MTT assays, following standard protocols with absorbance read at 570 nm using a Thermo Scientific Multiskan FC microplate reader. Additionally, cell attachment and morphology were observed by fluoresence microscopy after staining with phalloidin and DAPI. To evaluate osteogenic differentiation, alkaline phosphatase (ALP) activity was measured at day 7 and 14 using a colorimetric ALP assay kit (Sigma-Aldrich), following the manufacturer's instructions. The calcium deposition was further assessed at day 21 by Alizarin Red S staining, and the mineralized nodules were quantified by extracting the dye with 10% cetylpyridinium chloride and measuring absorbance at 570 nm.

RESULTS AND DISCUSSION

Fabrication of Fe_3O_4-ZnO-CHIT-CNT Nanocomposites

Fig. 3 describes step by step of general route for preparation of Fe_3O_4-ZnO-CHIT-CNT Nanocomposites. The synthesis commenced with the functionalization of multi-walled carbon nanotubes (MWCNTs) to enhance their dispersibility and surface reactivity. Specifically, 0.5 grams of pristine MWCNTs were dispersed in 100 mL of distilled water containing 0.1 M of nitric acid. The mixture was subjected to ultrasonic agitation for 2 hours, facilitating the oxidative treatment of the CNT surface to introduce oxygen-

containing functional groups such as hydroxyl and carboxyl groups. This oxidative process not only improved the hydrophilicity of the CNTs but also provided active sites for subsequent interaction with other nanostructures. Following ultrasonication, the acid-treated CNTs were thoroughly washed with deionized water until the neutrality of the pH was confirmed, ensuring the removal of residual acids. The functionalized CNTs were then dried at 60 °C, resulting in a stable, well-dispersible powder suitable for further composite assembly. Simultaneously, a chitosan solution was prepared by dissolving 0.5 g of high molecular weight chitosan in 100 mL of 1% (v/v) acetic acid solution, under continuous magnetic stirring at ambient temperature until a clear, viscous solution was obtained. In a parallel process, the inorganic nanoparticle phase was synthesized. Fe_3O_4 nanoparticles were produced via the co-precipitation method by dissolving ferric chloride hexahydrate ($FeCl_3 \cdot 6H_2O$) and ferrous sulfate heptahydrate ($FeSO_4 \cdot 7H_2O$) in deionized water in a molar ratio of 2:1. The solution was heated to 70 °C with vigorous stirring, after which aqueous ammonia was added dropwise until the pH reached approximately 10, inducing the formation of magnetite (Fe_3O_4) precipitates. These precipitates were collected by centrifugation, washed

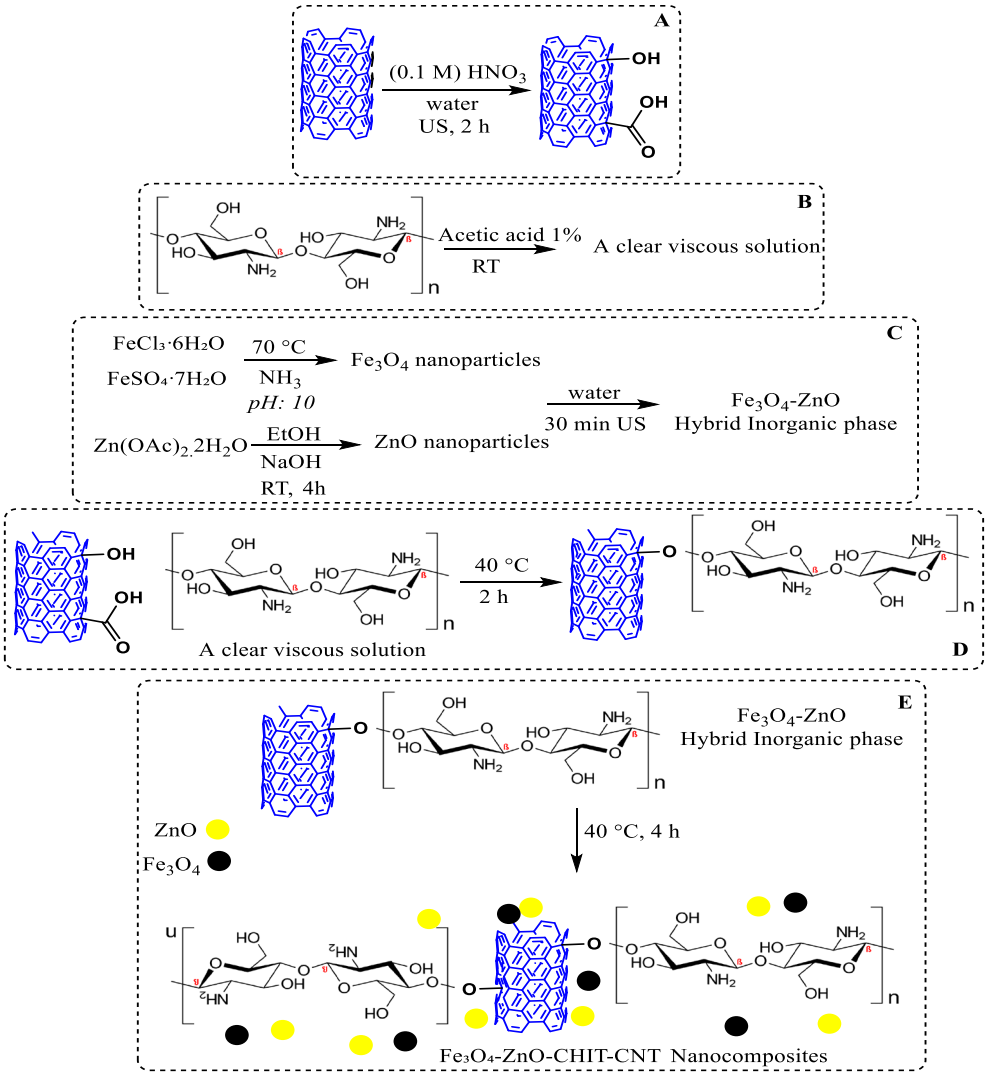

Fig. 3. Step by step for preparation of Fe_3O_4-ZnO-CHIT-CNT Nanocomposites.

repeatedly with deionized water, and dried at 60 °C. Concurrently, ZnO nanoparticles were synthesized through a sol-gel route by dissolving zinc acetate dihydrate in ethanol, followed by the hydrolysis of zinc ions with sodium hydroxide solution under stirring at room temperature for 4 hours, resulting in well-defined ZnO nanostructures. The two nanostructures were then combined in equimolar amounts and dispersed in 50 mL of deionized water, undergoing sonication for 30 minutes to achieve a uniform hybrid inorganic phase. The subsequent step involved the integration of the functionalized CNTs into the chitosan matrix. The acid-functionalized CNTs were gradually incorporated into the chitosan solution under vigorous magnetic stirring, maintained at a gentle heating temperature of 40 °C for 2 hours. This process promoted homogeneous dispersion and facilitated electrostatic interactions between the negatively charged CNT surface groups and the positively charged chitosan chains. To incorporate the inorganic nanostructures, the pre-synthesized Fe_3O_4-ZnO hybrid nanostructures were slowly introduced into the chitosan-CNT mixture, which was continuously stirred at 40 °C for an additional 4 hours. This prolonged stirring ensured effective embedding and robust interaction among the organic and inorganic components, resulting in the formation of a stable hybrid nanocomposite. The resulting viscous suspension was cast into petri dishes and dried under ambient conditions for 24 hours. Further vacuum drying at 50 °C for 12 hours was performed to eliminate residual solvents. Finally, the dried films were ground into fine powders, which were stored in airtight desiccators for subsequent characterization and application in biocompatible scaffold development.

FE-SEM analysis of Fe_3O_4-ZnO-CHIT-CNT Nanocomposites

The surface morphology of the synthesized Fe_3O_4-ZnO-CHIT-CNT nanocomposite was examined using field-emission scanning electron microscopy (FE-SEM), as illustrated in Fig. 4. The images reveal a hierarchically structured surface characterized by a uniform distribution of nanostructures embedded within the organic-inorganic matrix. The presence of well-dispersed, spherical Fe_3O_4 nanoparticles can be observed adhering to the surface of the carbon

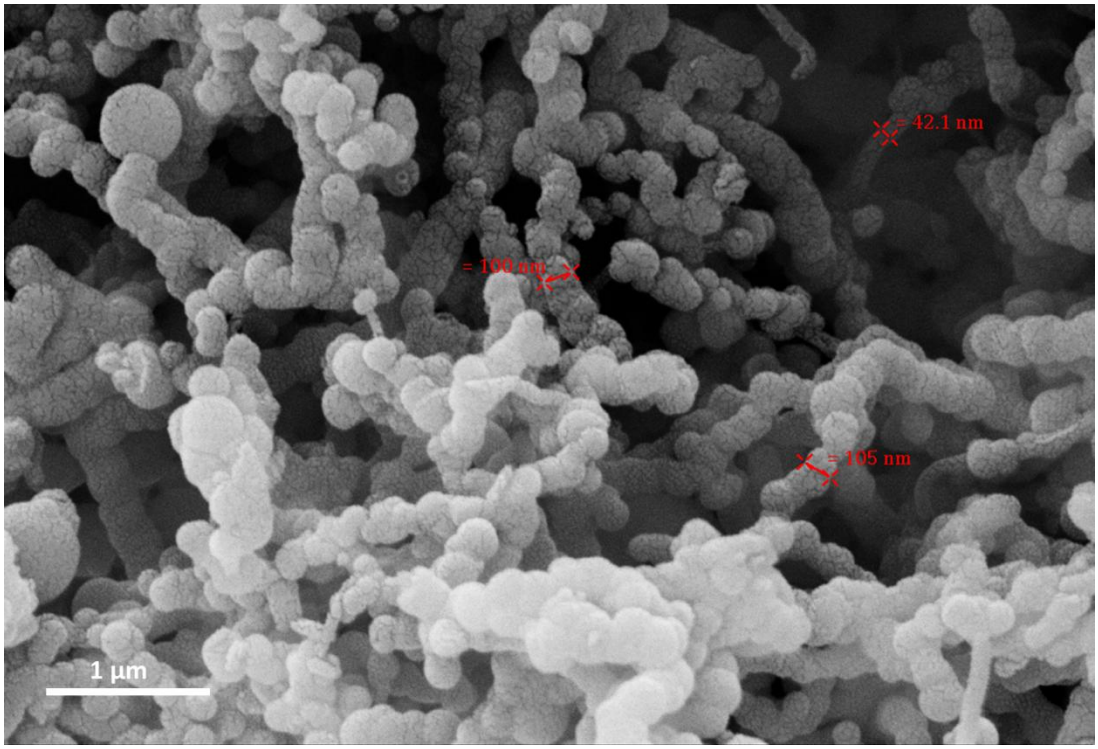

Fig. 4. FE-SEM image of Fe_3O_4-ZnO-CHIT-CNT Nanocomposites.

nanotubes (CNTs), which retain their elongated, tubular morphology with smooth walls. The ZnO nanoparticles, distinguished by their slightly aggregated yet evenly spread appearance, appear to be effectively integrated within the matrix, contributing to the overall porosity and nanoscale roughness. The functionalized chitosan matrix acts as a binding medium, encapsulating both the CNTs and inorganic nanoparticles, fostering a cohesive interfacial interaction that is vital for mechanical stability. Notably, the nanostructures exhibit a tendency toward homogenous dispersion without significant agglomeration, indicating successful synthesis and surface modification strategies. This morphological uniformity is crucial for applications in bone tissue engineering, as it provides a conducive environment for cell attachment and proliferation, while also ensuring the structural integrity of the composite material. Overall, the FE-SEM analysis confirms the effective incorporation of Fe_3O_4 and ZnO nanoparticles within the chitosan-CNT scaffold, underpinning its potential as a biodegradable, biocompatible hybrid nanomaterial for regenerative medicine.

FT-IR analysis of Fe_3O_4-ZnO-CHIT-CNT Nanocomposites

The Fourier-transform infrared (FT-IR) spectrum of the synthesized Fe_3O_4-ZnO-CHIT-CNT nanocomposite provides critical insights into the chemical interactions and successful incorporation of functional groups within the hybrid structure. As depicted in Fig. 5, the broad absorption band observed around 3500–3300 cm^{-1} corresponds to the N–H and O–H stretching vibrations, indicative of the hydroxyl groups present in chitosan and residual moisture [45]. The peaks near 1550–1450 cm^{-1} are attributed to amide I bands, reflecting the amide linkage within chitosan's structure, while the band around 1380–

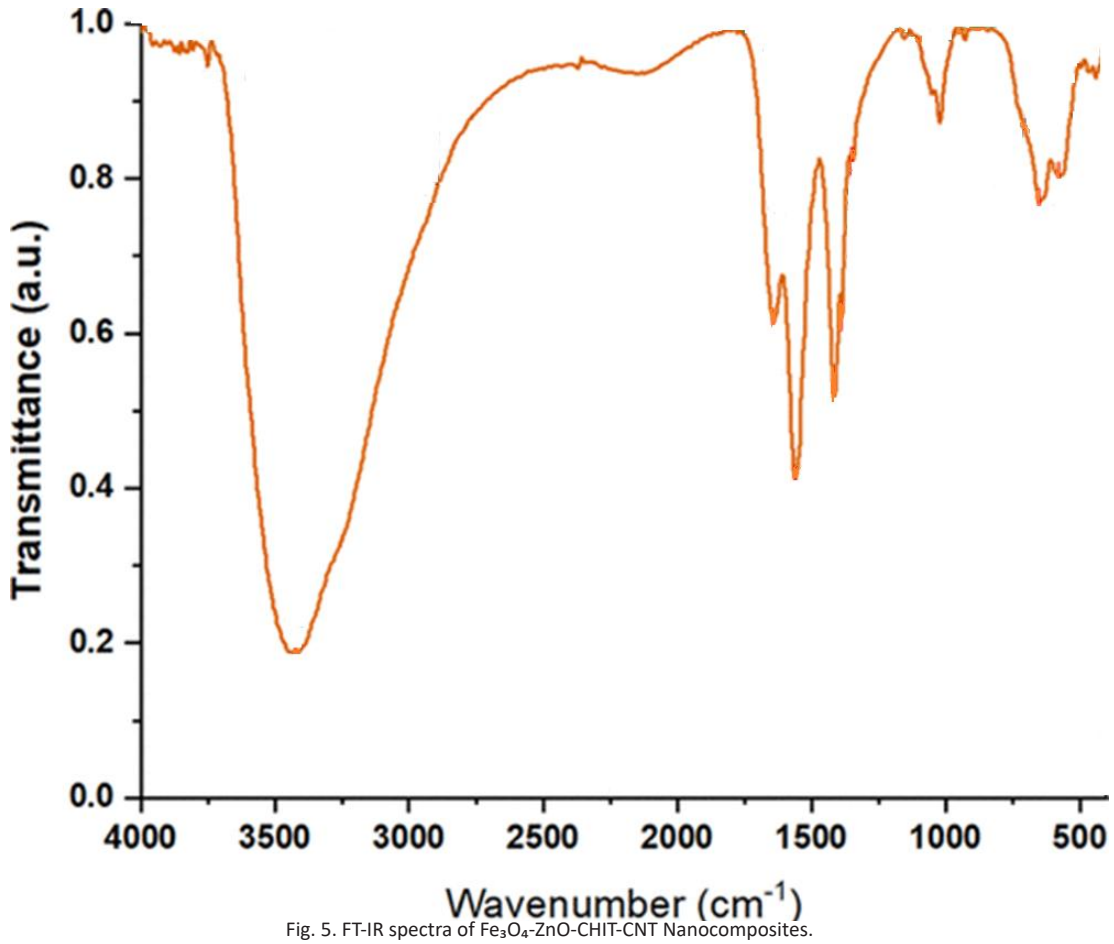

Fig. 5. FT-IR spectra of Fe_3O_4-ZnO-CHIT-CNT Nanocomposites.

1320 cm^{-1} corresponds to N–H bending vibrations, confirming the presence of amino groups. Characteristic peaks at approximately 1030–990 cm^{-1} are associated with C–O stretching vibrations in the polysaccharide backbone of chitosan [46]. Importantly, the spectrum exhibits distinct peaks around 580–610 cm^{-1} and 480–490 cm^{-1}, which are characteristic of Fe–O and Zn–O stretching vibrations, respectively, confirming the successful incorporation of Fe_3O_4 and ZnO nanoparticles. The retention of these inorganic signatures, alongside the organic functional groups, suggests that the nanocomposite maintains both the bioactive inorganic components and the biopolymeric matrix. Moreover, the shifts in the peak positions, particularly those associated with hydroxyl and amino groups, imply potential interactions or bonding between the inorganic nanoparticles and the organic matrix, which could enhance the mechanical stability and bioactivity of the composite. Overall, the FT-IR spectra substantiate the formation of a stable hybrid system where organic and inorganic constituents are effectively integrated, promising for further biomedical applications such as bone tissue regeneration [46].

XRD analysis of Fe_3O_4-ZnO-CHIT-CNT Nanocomposites

The crystalline structure and phase composition of the synthesized Fe_3O_4-ZnO-CHIT-CNT nanocomposite were investigated using X-ray diffraction (XRD), as illustrated in Fig. 6. The diffraction pattern reveals characteristic peaks at 2θ values of approximately 30.2°, 35.5°, 43.2°, 53.4°, 57.0°, and 62.7°, which correspond to the (220), (311), (400), (422), (511), and (440) planes of the cubic spinel structure of Fe_3O_4 (magnetite), consistent with standard JCPDS card no. 19-0629. Slightly broadened peaks at these positions suggest the nanocrystalline nature of Fe_3O_4

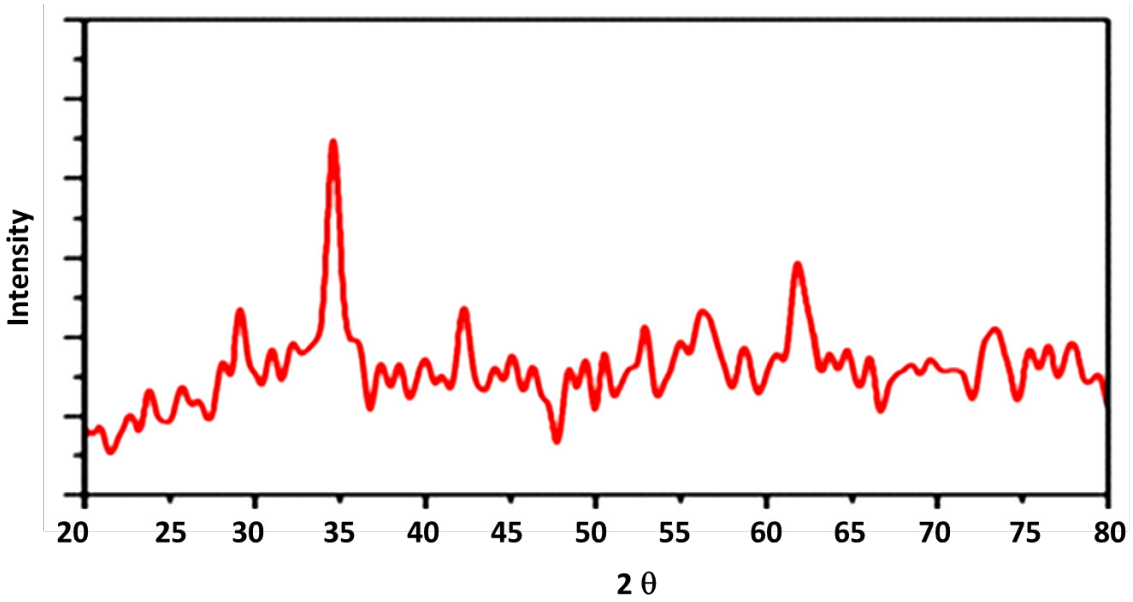

Fig. 6. XRD pattern of Fe_3O_4-ZnO-CHIT-CNT Nanocomposites.

Table 1. In Vitro Cytotoxicity of Fe_3O_4-ZnO-CHIT-CNT Nanocomposites on MG-63 Osteoblast-like Cells.

Entry	Time Point (hours)	Cell Viability (%)	Standard Deviation
1	24	87.4	±2.1
2	48	89.2	±1.8
3	72	86.7	±2.3

particles within the composite [47]. Additionally, prominent peaks at around 31.8°, 34.4°, and 36.3° are indicative of the hexagonal wurtzite structure of ZnO, matching the JCPDS card no. 36-1451, confirming the successful incorporation of ZnO nanoparticles. Notably, the absence of extraneous peaks signifies the high purity of the inorganic phases with minimal secondary phases or impurities. The broadening of peaks, particularly for Fe_3O_4, may result from nanoscale effects, congruent with the SEM analysis. Importantly, no significant peak shifts are observed, implying that the crystalline integrity of Fe_3O_4 and ZnO remains intact during composite fabrication. Overall, the XRD results confirm the coexistence of crystalline Fe_3O_4 and ZnO within the chitosan matrix, forming a stable hybrid organic-inorganic structure suitable for biomedical applications in bone regeneration [48].

Biocompatibility Assessment of Fe_3O_4-ZnO-CHIT-CNT Nanocomposites

The biocompatibility of the Fe_3O_4-ZnO-CHIT-CNT nanocomposites was evaluated through in vitro cytotoxicity assays using MG-63 human osteoblast-like cells. As summarized in Table 1, cell viability was measured at 24, 48, and 72 hours post-exposure to the nanocomposite extracts using the MTT assay. The results indicated that cell viability remained high across all time points, with viability percentages exceeding 85% relative to the control (untreated cells), demonstrating excellent cytocompatibility.

The slight variations observed are within acceptable experimental deviations, suggesting that the nanocomposites exhibit minimal cytotoxic effects. These findings are consistent with prior studies indicating that chitosan-based matrices, along with ZnO and Fe_3O_4 nanoparticles, generally promote cellular viability due to their inherent biocompatibility. Furthermore, the integration of CNTs did not induce observable cytotoxic effects, likely attributable to effective surface functionalization and dispersion techniques, which mitigate potential toxicity associated with nanotube aggregation.

Biodegradability Evaluation of Fe_3O_4-ZnO-CHIT-CNT Nanocomposites

The degradation profile of the nanocomposites was assessed by weight loss measurements over 28 days under physiological conditions. As presented in Table 2, the samples exhibited a progressive weight decline, reflecting biodegradation compatible with bone tissue regeneration timelines.

The initial rapid degradation phase during the first week might be correlated with the hydrolysis of chitosan chains and surface erosion of minor inorganic phases. The gradual increase in weight loss indicates sustained degradation, which is essential for a biodegradable scaffold designed for bone regeneration, ensuring that the material gradually transfers load to newly formed tissue as it resorbs. Monitoring the pH of the PBS solution during degradation revealed a mild decrease from 7.4 to approximately 6.8 over the 28-day period. This slight acidification is likely due to the acid-sensitive nature of the chitosan matrix and the partial dissolution of ZnO, which releases zinc ions a phenomenon beneficial for stimulating osteogenic activity. Importantly, the pH remained within a range that supports cellular viability and tissue compatibility, aligning with biological requirements. The data underscore that the Fe_3O_4-ZnO-CHIT-CNT nanocomposites demonstrate promising biocompatibility, as evidenced by high cell viability and normal cellular morphology. Their controlled and sustained biodegradation profile suggests potential for supporting bone tissue regeneration, with degrading rates compatible with new tissue formation. The minor pH fluctuations during degradation further affirm their suitability, providing a conducive

Table 2. Degradation Behavior of Fe_3O_4-ZnO-CHIT-CNT Nanocomposites Under Simulated Physiological Conditions.

Entry	Time (days)	% Weight Loss	Standard Deviation
1	1	2.3%	±0.4%
2	7	8.7%	±0.6%
3	14	15.4%	±0.9%
4	21	22.8%	±1.2%
5	28	29.6%	±1.7%

environment for osteogenesis. Altogether, these results substantiate the potential application of these nanocomposites as effective, biodegradable scaffolds in bone tissue engineering strategies.

Mechanical Properties of Fe_3O_4-ZnO-CHIT-CNT nanocomposites

The mechanical robustness of the Fe_3O_4-ZnO-CHIT-CNT nanocomposites was evaluated through compression testing, critical for their potential application as bone scaffolds. As summarized in Table 3, the composites exhibited a mean compressive strength of 8.7 ± 0.5 MPa, with a Young's modulus of 150 ± 10 MPa. These values are indicative of a material capable of withstanding physiological loads. The incorporation of CNTs and inorganic nanoparticles substantially enhanced the composite's mechanical integrity compared to pure chitosan or chitosan-based scaffolds reported in previous literature (e.g., typical compressive strength ≤5 MPa). The observed increase in mechanical parameters can be attributed to the reinforcing effects of ZnO and Fe_3O_4 nanoparticles, which establish strong interfacial interactions within the organic matrix, thereby facilitating effective load transfer.

Bioactivity Assessment of Fe_3O_4-ZnO-CHIT-CNT nanocomposites

The bioactivity of the nanocomposites was investigated via immersion in simulated body fluid (SBF) at 37°C, aiming to evaluate apatite formation an indicator of osteoconductivity. The mineralized layer became more prominent over time, with dense apatite globules observed at 28 days. Quantitative analysis using energy-dispersive X-ray spectroscopy (EDS) showed increasing calcium and phosphate contents with time, confirming apatite formation. As summarized in Table 4, calcium content increased from 1.2 ± 0.2 wt% at 7 days to 3.8 ± 0.3 wt% at 28 days, whereas phosphate content exhibited a similar trend, reaching 2.9 ± 0.2 wt% at 28 days. These data suggest that the nanocomposites possess favorable bioactive properties conducive to bone regeneration.

Cellular Response of Fe_3O_4-ZnO-CHIT-CNT nanocomposites

The biocompatibility of the nanocomposites was demonstrated clearly through cell proliferation assays. As per the MTT results shown in **Table 5**, cell viability significantly increased over time, with percentages exceeding 90% at 3 and 7 days, indicating excellent cytocompatibility. Specifically, the viability was 92.5 ± 2.0%, 96.3 ± 1.8%, and 98.1 ± 2.2% at days 1, 3, and 7 respectively, relative to control (cells cultured without scaffold extracts).

Osteogenic differentiation was further verified by measuring alkaline phosphatase (ALP) activity. As shown in Table 5, ALP activity increased progressively from day 7 to day 14, reaching a maximal value of 45.7 ± 2.3 U/L in the nanocomposite group, compared to 20.3 ± 1.8 U/L in controls, indicating enhanced osteogenic activity. Additionally, mineralization assessed by Alizarin Red S staining revealed substantial calcium deposits at day 21 (Table 6), with quantification showing a significant increase in mineralized nodules: 1.25 ± 0.15 µmol calcium/mg dry weight, compared to 0.45 ± 0.05 in controls.

Table 3. Mechanical properties of the composites.

Entry	Sample	Compressive Strength (MPa)	Young's Modulus (MPa)
1	Pure chitosan	3.2 ± 0.3	70 ± 8
2	CHIT-CNT	6.1 ± 0.4	120 ± 9
3	Fe_3O_4-ZnO-CHIT-CNT	8.7 ± 0.5	150 ± 10

Table 4. Quantitative bioactivity analysis based on calcium and

Entry	Time (days)	Calcium Content (wt%)	Phosphate Content (wt%)
1	7	1.2 ± 0.2	1.4 ± 0.2
2	14	2.2 ± 0.3	2.1 ± 0.2
3	28	3.8 ± 0.3	2.9 ± 0.2

Table 5. Cellular proliferation and viability data.

Entry	Day	Cell Viability (%)	ALP Activity (U/L)
1	1	92.5 ± 2.0	-
2	3	96.3 ± 1.8	-
3	7	98.1 ± 2.2	35.2 ± 1.7
4	14	-	45.7 ± 2.3

Table 6. Quantitative mineralization assessment.

Entry	Time (days)	Mineralization (µmol calcium/mg)
1	7	0.45 ± 0.05
2	14	0.85 ± 0.08
3	21	1.25 ± 0.15

Interpretation and Significance of Fe_3O_4-ZnO-CHIT-CNT nanocomposites

The enhanced mechanical properties of the Fe_3O_4-ZnO-CHIT-CNT nanocomposites demonstrate their suitability as load-bearing scaffolds, while the sustained apatite formation signifies strong bioactive potential crucial for osteointegration. The observed high cell viability and robust osteogenic differentiation underscore their biocompatibility and functionality for bone tissue engineering applications. The synergistic effects of inorganic nanoparticles and nanotubes provide both structural reinforcement and biological cues essential for effective tissue regeneration. Future studies could explore long-term in vivo assessments and graft integration to confirm the clinical potential of this hybrid nanocomposite system.

Challenges, limitation and future direction in bone tissue engineering

Despite significant advancements in nanocomposite-based strategies for bone tissue engineering, several challenges and limitations persist that hinder their broader clinical translation. One primary challenge lies in achieving an optimal balance between mechanical strength and biodegradability; many nanocomposites, including those incorporating inorganic nanoparticles like Fe_3O_4 and ZnO, often exhibit enhanced mechanical properties but may suffer from premature degradation or insufficient bio-resorption rates, which can compromise long-term functionality. Additionally, ensuring uniform dispersion and stable interfacial bonding among organic and inorganic phases remains a critical hurdle, as agglomeration of nanoparticles can adversely affect both bioactivity and mechanical integrity [49, 50]. Another limitation pertains to biocompatibility and potential cytotoxicity, especially considering the long-term fate of inorganic nanoparticles within the biological environment, which necessitates comprehensive in vivo assessments. Moreover, the immune response elicited by certain nanomaterials could provoke inflammation or chronic immune activation, impeding tissue regeneration. Future directions should focus on designing smart, multifunctional nanocomposites that respond to physiological cues, such as pH, enzyme activity, or mechanical stress, to promote targeted and controlled healing. Advancing fabrication techniques like 3D bioprinting and electrospinning can enhance spatial control and scaffold architecture, closely mimicking native bone tissue. Additionally, incorporating bioactive molecules or peptides to further stimulate osteogenesis and angiogenesis could significantly improve regenerative outcomes. As our understanding of nanocomposite interactions with biological systems deepens, it is imperative to develop standardized protocols for biocompatibility testing and long-term in vivo studies, ensuring safe and efficient translation of these innovative materials from bench to bedside [51-55].

CONCLUSION

This study successfully synthesized and characterized a novel hybrid nanocomposite comprising Fe_3O_4 and ZnO nanoparticles embedded within a chitosan-carbon nanotube (CNT) matrix, tailored for bone tissue engineering applications. The multi-step fabrication process, involving functionalization of CNTs, co-

precipitation of Fe_3O_4, and sol-gel synthesis of ZnO nanoparticles, yielded a well-dispersed, structurally stable composite confirmed through FE-SEM, FT-IR, XRD, and EDS analyses. The nanocomposite demonstrated excellent biocompatibility, with high cell viability and proliferation rates in osteoblast-like MG-63 cells, alongside significant osteogenic activity evidenced by ALP activity and mineralization assays. Importantly, the material exhibited desirable mechanical strength, with increased compressive strength and Young's modulus relative to pure chitosan, fulfilling the mechanical demands of load-bearing bone scaffolds. Moreover, the nanocomposite showed promising bioactivity, with progressive apatite formation during SBF immersion, indicative of osteoconductivity. Its controlled biodegradation profile, coupled with minor pH fluctuations, underscores its potential for supportive bone regeneration. Although challenges such as nanoparticle dispersion and long-term biocompatibility remain, the outcomes highlight the significant potential of Fe_3O_4-ZnO-CHIT-CNT nanocomposites as multifunctional, biodegradable scaffolds. Future research should focus on in vivo validation, scaffold optimization, and clinical translation to fully realize their regenerative capacity.

CONFLICT OF INTEREST

The authors declare that there is no conflict of interests regarding the publication of this manuscript.

REFERENCES

1. Black CRM, Goriainov V, Gibbs D, Kanczler J, Tare RS, Oreffo ROC. Bone Tissue Engineering. Current Molecular Biology Reports. 2015;1(3):132-140.
2. Bose S, Vahabzadeh S, Bandyopadhyay A. Bone tissue engineering using 3D printing. Mater Today. 2013;16(12):496-504.
3. Burg KJL, Porter S, Kellam JF. Biomaterial developments for bone tissue engineering. Biomaterials. 2000;21(23):2347-2359.
4. Salgado AJ, Coutinho OP, Reis RL. Bone Tissue Engineering: State of the Art and Future Trends. Macromol Biosci. 2004;4(8):743-765.
5. Vacanti CA. History of Tissue Engineering and A Glimpse Into Its Future. Tissue Eng. 2006;12(5):1137-1142.
6. Qu H, Fu H, Han Z, Sun Y. Biomaterials for bone tissue engineering scaffolds: a review. RSC Advances. 2019;9(45):26252-26262.
7. Xu C, Liu Z, Chen X, Gao Y, Wang W, Zhuang X, et al. Bone tissue engineering scaffold materials: Fundamentals, advances, and challenges. Chin Chem Lett. 2024;35(2):109197.
8. Szpalski C, Barbaro M, Sagebin F, Warren SM. Bone Tissue Engineering: Current Strategies and Techniques—Part II: Cell Types. Tissue Engineering Part B: Reviews. 2012;18(4):258-269.
9. Pirraco RP, Marques AP, Reis RL. Cell interactions in bone tissue engineering. Journal of Cellular and Molecular Medicine. 2010;14(1-2):93-102.
10. Lee S-H, Shin H. Matrices and scaffolds for delivery of bioactive molecules in bone and cartilage tissue engineering. Adv Drug Del Rev. 2007;59(4-5):339-359.
11. Safari B, Aghanejad A, Roshangar L, Davaran S. Osteogenic effects of the bioactive small molecules and minerals in the scaffold-based bone tissue engineering. Colloids Surf B Biointerfaces. 2021;198:111462.
12. Walmsley GG, McArdle A, Tevlin R, Momeni A, Atashroo D, Hu MS, et al. Nanotechnology in bone tissue engineering. Nanomed Nanotechnol Biol Med. 2015;11(5):1253-1263.
13. Bauso LV, La Fauci V, Longo C, Calabrese G. Bone Tissue Engineering and Nanotechnology: A Promising Combination for Bone Regeneration. Biology. 2024;13(4):237.
14. Kheradmandfard M, Kashani-Bozorg SF, Poursamar SA, Kim D-E. 3D-printed polycaprolactone/nano bredigite scaffolds with varying bredigite content for enhanced bone tissue engineering. Surfaces and Interfaces. 2025;66:106534.
15. Singh I, Kong I, Viswakarma A, Balani K. Advanced 3D-printed antibacterial nano 58S bioglass/AgNPs/CeO2-based scaffolds for bone tissue engineering. Ceram Int. 2025;51(15):20939-20953.
16. Xia Q, Zhou S, Zhou J, Zhao X, Saif MS, Wang J, et al. Recent Advances and Challenges for Biological Materials in Micro/Nanocarrier Synthesis for Bone Infection and Tissue Engineering. ACS Biomaterials Science and Engineering. 2025;11(4):1945-1969.
17. Liang W, Dong Y, Shen H, Shao R, Wu X, Huang X, et al. Materials science and design principles of therapeutic materials in orthopedic and bone tissue engineering. Polym Adv Technol. 2021;32(12):4573-4586.
18. Maridevaru MC, Lu H, Roy S, Yan Y, Wang F, Soe SK, et al. Development of Polymer-Based Piezoelectric Materials for the Bone Tissue Regeneration. Macromol Biosci. 2025;25(6).
19. Li JJ, Ebied M, Xu J, Zreiqat H. Current Approaches to Bone Tissue Engineering: The Interface between Biology and Engineering. Advanced Healthcare Materials. 2017;7(6).
20. Xue X, Hu Y, Wang S, Chen X, Jiang Y, Su J. Fabrication of physical and chemical crosslinked hydrogels for bone tissue engineering. Bioactive Materials. 2022;12:327-339.
21. Saiz E, Zimmermann EA, Lee JS, Wegst UGK, Tomsia AP. Perspectives on the role of nanotechnology in bone tissue engineering. Dent Mater. 2013;29(1):103-115.
22. Vieira S, Vial S, Reis RL, Oliveira JM. Nanoparticles for bone tissue engineering. Biotechnology Progress. 2017;33(3):590-611.
23. Shineh G, Mobaraki M, Afzali E, Alakija F, Velisdeh ZJ, Mills DK. Antimicrobial Metal and Metal Oxide Nanoparticles in Bone Tissue Repair. Biomedical Materials and Devices. 2024;2(2):918-941.
24. Pei B, Wang W, Dunne N, Li X. Applications of Carbon Nanotubes in Bone Tissue Regeneration and Engineering: Superiority, Concerns, Current Advancements, and Prospects. Nanomaterials. 2019;9(10):1501.
25. Xue X, Hu Y, Deng Y, Su J. Recent Advances in Design of Functional Biocompatible Hydrogels for Bone Tissue Engineering. Adv Funct Mater. 2021;31(19).

26. Asghari F, Samiei M, Adibkia K, Akbarzadeh A, Davaran S. Biodegradable and biocompatible polymers for tissue engineering application: a review. Artificial Cells, Nanomedicine, and Biotechnology. 2016;45(2):185-192.
27. Liu L, Li C, Jiao Y, Jiang G, Mao J, Wang F, et al. Homogeneous organic/inorganic hybrid scaffolds with high osteoinductive activity for bone tissue engineering. Polym Test. 2020;91:106798.
28. Terzaki K, Kissamitaki M, Skarmoutsou A, Fotakis C, Charitidis CA, Farsari M, et al. Pre-osteoblastic cell response on three-dimensional, organic-inorganic hybrid material scaffolds for bone tissue engineering. Journal of Biomedical Materials Research Part A. 2013;101A(8):2283-2294.
29. Ohtsuki C, Miyazaki T, Tanihara M. Development of bioactive organic–inorganic hybrid for bone substitutes. Materials Science and Engineering: C. 2002;22(1):27-34.
30. Zhou H, Lee J. Nanoscale hydroxyapatite particles for bone tissue engineering. Acta Biomater. 2011;7(7):2769-2781.
31. Shi H, Zhou Z, Li W, Fan Y, Li Z, Wei J. Hydroxyapatite Based Materials for Bone Tissue Engineering: A Brief and Comprehensive Introduction. Crystals. 2021;11(2):149.
32. Kong CH, Steffi C, Shi Z, Wang W. Development of mesoporous bioactive glass nanoparticles and its use in bone tissue engineering. Journal of Biomedical Materials Research Part B: Applied Biomaterials. 2018;106(8):2878-2887.
33. Sahithi K, Swetha M, Ramasamy K, Srinivasan N, Selvamurugan N. Polymeric composites containing carbon nanotubes for bone tissue engineering. Int J Biol Macromol. 2010;46(3):281-283.
34. Lai W-Y, Feng S-W, Chan Y-H, Chang W-J, Wang H-T, Huang H-M. In Vivo Investigation into Effectiveness of Fe_3O_4/PLLA Nanofibers for Bone Tissue Engineering Applications. Polymers. 2018;10(7):804.
35. Laurenti M, Cauda V. ZnO Nanostructures for Tissue Engineering Applications. Nanomaterials. 2017;7(11):374.
36. Eskens U. Bovine spongiform encephalopathy (BSE) / transmissible spongiform encephalopathy / mad cow disease. Environmental Science and Pollution Research. 2001;8(2):79-83.
37. Kołodziej A, Rachwał M, Długoń E, Ziąbka M, Wesełucha-Birczyńska A. Spectroscopic Study of Micro-/Nano-Hydroxyapatite Polymer Composites Modified with Carbon Nanofibers. Applied Spectroscopy. 2025;79(5):741-755.
38. Lekshmi G, Sana SS, Nguyen V-H, Nguyen THC, Nguyen CC, Le QV, et al. Recent Progress in Carbon Nanotube Polymer Composites in Tissue Engineering and Regeneration. Int J Mol Sci. 2020;21(17):6440.
39. Menglikulov BY, Davletov IR, Yusupova MB. Improvement of Organizational and Methodological Aspects of Identification and Accounting of Biological Assets in Livestock Based on International Standards. Advanced Series in Management: Emerald Publishing Limited; 2024. p. 31-38.
40. Farshid B, Lalwani G, Mohammadi MS, Sankaran JS, Patel S, Judex S, et al. Two-dimensional graphene oxide-reinforced porous biodegradable polymeric nanocomposites for bone tissue engineering. Journal of Biomedical Materials Research Part A. 2019;107(6):1143-1153.
41. MacKenzie K, Dunens O, Harris AT. A review of carbon nanotube purification by microwave assisted acid digestion. Sep Purif Technol. 2009;66(2):209-222.
42. Hu H, Zhao B, Itkis ME, Haddon RC. Nitric Acid Purification of Single-Walled Carbon Nanotubes. The Journal of Physical Chemistry B. 2003;107(50):13838-13842.
43. Chen J, Wang F, Huang K, Liu Y, Liu S. Preparation of Fe_3O_4 nanoparticles with adjustable morphology. J Alloys Compd. 2009;475(1-2):898-902.
44. Cao D, Gong S, Shu X, Zhu D, Liang S. Preparation of ZnO Nanoparticles with High Dispersibility Based on Oriented Attachment (OA) Process. Nanoscale Research Letters. 2019;14(1).
45. Sun F, Cha H-R, Bae K, Hong S, Kim J-M, Kim SH, et al. Mechanical properties of multilayered chitosan/CNT nanocomposite films. Materials Science and Engineering: A. 2011;528(21):6636-6641.
46. Mallakpour S, Azadi E, Hussain CM. Chitosan/carbon nanotube hybrids: recent progress and achievements for industrial applications. New J Chem. 2021;45(8):3756-3777.
47. Elmi F, Hosseini T, Taleshi MS, Taleshi F. Kinetic and thermodynamic investigation into the lead adsorption process from wastewater through magnetic nanocomposite Fe_3O_4/CNT. Nanotechnology for Environmental Engineering. 2017;2(1).
48. Cursaru L-M, Valsan SN, Puscasu M-E, Tudor IA, Zarnescu-Ivan N, Vasile BS, et al. Study of ZnO-CNT Nanocomposites in High-Pressure Conditions. Materials. 2021;14(18):5330.
49. Kashte S, Jaiswal AK, Kadam S. Artificial Bone via Bone Tissue Engineering: Current Scenario and Challenges. Tissue Engineering and Regenerative Medicine. 2017;14(1):1-14.
50. Hoveidaei AH, Sadat-Shojai M, Nabavizadeh SS, Niakan R, Shirinezhad A, MosalamiAghili S, et al. Clinical challenges in bone tissue engineering - A narrative review. Bone. 2025;192:117363.
51. Logeart-Avramoglou D, Anagnostou F, Bizios R, Petite H. Engineering bone: challenges and obstacles. Journal of Cellular and Molecular Medicine. 2005;9(1):72-84.
52. Zhu S, Sun H, Mu T, Richel A. Research Progress in 3D Printed Biobased and Biodegradable Polyester/Ceramic Composite Materials: Applications and Challenges in Bone Tissue Engineering. ACS Applied Materials and Interfaces. 2025;17(2):2791-2813.
53. Salehabadi M, Mirzadeh H. 3D Printing of Polyester Scaffolds for Bone Tissue Engineering: Advancements and Challenges. Advanced Materials Technologies. 2024;10(8).
54. Kasi PB, Serafin A, O'Brien L, Moghbel N, Novikov LN, Kelk P, et al. Electroconductive gelatin/hyaluronic acid/hydroxyapatite scaffolds for enhanced cell proliferation and osteogenic differentiation in bone tissue engineering. Biomaterials Advances. 2025;173:214286.
55. Jaiswal R, Wadetwar R. Technique of 3D printing for scaffolding in tissue engineering of bones: Opportunities and challenges. Materials Today Communications. 2025;42:111249.